A BODIPY-based 'turn-on' fluorescent probe for hypoxic cells imaging

Sisi Wang, Hui Liu, John Mack, Jiangwei Tian, Bin Zou, Hua Lu,* Zhifang Li,

Jianxiong Jiang and Zhen Shen*

I. Experimental section

II. Supplementary Figure

III. References

IV. ¹H NMR

I. Experimental Section

I.1 Materials and instrumentations

All reagents were obtained from commercial suppliers and used without further purification unless otherwise indicated.   Glassware was dried in an oven at 100 °C and cooled under a stream of inert gas before use.   ^{1}H NMR spectra were recorded on a Bruker DRX400 spectrometer and referenced to the residual proton signals of the solvent.   MALDI-TOF-MS were recorded on a Bruker Daltonics microTOF-Q II spectrometer.   All the solvents employed for the spectroscopic measurements were of spectroscopic grade (Aldrich).

I.2 Synthesis and characterization

1a R_1=OH, R_2=NO$_2$
2a R_1=H, R_2=NO$_2$
3a R_1=NO$_2$. R_2=H

1b R_1=OH, R_2=NH$_2$
2b R_1=H, R_2=NH$_2$
3b R_1=NH$_2$. R_2=H
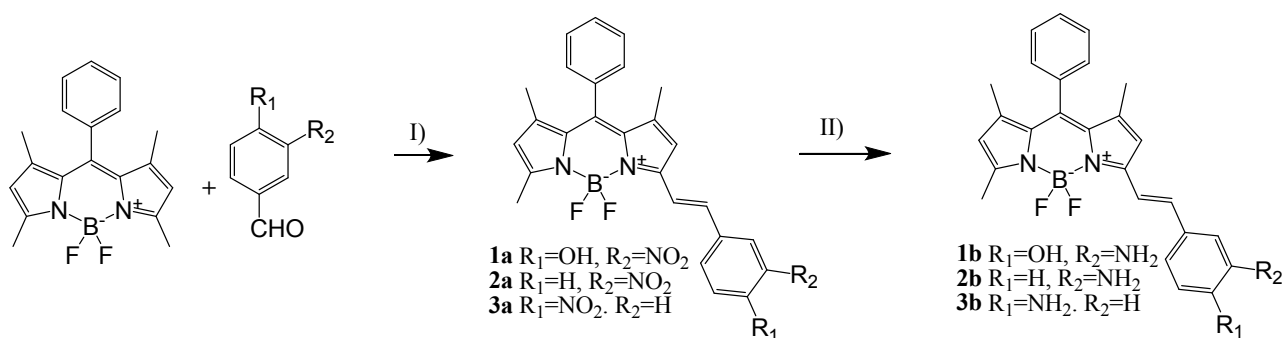
3-(4-hydroxy-3-nitro styryl)-BODIPY 1a

A solution of tetramethyl-BODIPY (162 mg, 0.5 mmol), 4-hydroxy-3-nitrobenzaldehyde (125 mg, 0.75 mmol) and a crystal of p-TsOH in a mixture of toluene (50 ml) and piperidine (1 mL) was placed in a round bottom flask equipped with a Dean Stark trap, the mixture was heated at its boiling point until it had evaporated to dryness. The resulting solid was dissoved in dichloromethane and washed with water three times.   The organic phase was dried over MgSO$_4$ and the solvent was evaporated under reduced pressure, and the resulting crude residue was purified by silica-gel flash column chromatography (25% ethyl acetate/hexane) and recrystallized from CH$_2$Cl$_2$/Hexane to provide **1a** as a purple solid (137 mg, 58%).   ^{1}H NMR (400 MHz, CDCl$_3$) δ = 10.70 (s, 1 H), 8.16 (s, 1 H), 7.94 (d, J = 12 Hz, 1 H), 7.60 (d, J = 16 Hz, 1 H), 7.50 (m, 3 H), 7.30 (d, J = 4 Hz, 2 H), 7.19 (d, J = 12 Hz, 1 H), 7.12 (d, J = 16 Hz, 1 H), 6.57 (s, 1 H), 6.04 (s, 1 H), 2.61 (s, 3 H), 1.43 (s, 3 H), 1.40 (s, 3 H);

Uv/vis (CH_2Cl_2), λ_{max} (ε) = 562 nm (86 300 dm^3 mol^{-1} cm^{-1});   HRMS-ESI: m/z: calcd $[C_{26}H_{22}BF_2N_3O_3Na]^+$ m/z = 496.1614, found m/z = 496.1625.

3-(4-hydroxy-3-amino styryl)-BODIPY 1b

3-(4-hydroxy-3-nitro styryl)-BODIPY **1a** (20 mg, 0.042 mmol) was dissolved in 9 mL of ethyl acetate, H_2O (7 mL), NH_4Cl (250 mg) and Fe (150 mg) were added and the reaction mixture was heated to reflux for 1h until TLC monitoring indicated complete consumption of the starting material.   After completion of the reaction, the precipitate was removed by filtration, the mixture was extracted with EtOAc (3 × 15 mL), the organic phase was washed with saturated $NaHCO_3$ and then dried over Na_2SO_4, concentrated under reduced pressure and purified by silica-gel flash column chromatography (50% ethyl acetate/hexane), recrystallized from CH_2Cl_2/Hexane to provide **1b** as dark-red crystals (16 mg, 86%). ^{1}H NMR (400 MHz, CD_2Cl_2) δ = 7.44-7.42 (m, 3 H), 7.35 (d, J = 16 Hz, 1 H), 7.26-7.24 (m, 2 H), 7.07 (d, J = 16 Hz, 1 H), 6.97 (s, 1 H), 6.79 (d, J = 8 Hz, 1 H), 6.66 (d, J = 8 Hz, 1 H), 6.53 (s, 2 H), 5.95 (s, 1 H), 2.47 (s, 3 H), 1.36 (s, 3 H), 1.18 (s, 3 H);   Uv/vis (CH_2Cl_2), λ_{max} (ε) = 575 nm (119 000 dm^3 mol^{-1} cm^{-1});   HRMS-ESI: m/z: calcd $[C_{26}H_{24}BF_2N_3ONa]^+$ m/z = 466.1873, found m/z = 466.1877.

Compounds **2a** and **3a** were obtained as purple powders by following a procedure similar to that of **1a** in 35% and 43% yield, respectively.   For **2a**: ^{1}H NMR (400 MHz, $CDCl_3$) δ = 8.32 (s, 1 H), 8.13 (d, J = 8 Hz, 1 H), 7.95 (d, J = 8 Hz, 1 H), 7.76 (d, J = 16 Hz, 1 H), 7.56-7.50 (m, 4 H), 7.32-7.30 (m, 2 H), 7.22 (d, J = 16 Hz, 1 H), 6.61 (s, 1 H), 6.06 (s, 1 H), 2.62 (s, 3 H), 1.44 (s, 3 H), 1.41 (s, 3 H); λ_{max} (ε) = 560 nm (137 000 dm^3 mol^{-1} cm^{-1}); HRMS-ESI: m/z: calcd $[C_{26}H_{22}BF_2N_3O_2Na]^+$ m/z = 480.1665, found m/z = 480.1674;   For **3a**: ^{1}H NMR (400 MHz, $CDCl_3$) δ = 8.22 (m, J = 8 Hz, 2 H), 7.80 (d, J = 8 Hz, 1 H), 7.69 (d, J = 8 Hz, 2 H), 7.52 (m, 3 H), 7.32 (m, 2 H), 7.19 (d, J = 16 Hz, 1 H), 6.62 (s, 1 H), 6.07 (s, 1 H), 2.62 (s, 3 H), 1.44 (s, 3 H), 1.42 (s, 3 H); λ_{max} (ε) = 572 nm (150 600 dm^3 mol^{-1} cm^{-1}); HRMS-ESI: m/z: calcd $[C_{26}H_{22}BF_2N_3O_2Na]^+$ m/z = 480.1665 ; found m/z = 480.1666.

Compounds **2b** and **3b** were obtained as purple crystals by following a procedure similar to that of **1b** in 81% and

89% yield, respectively.   For **2b**: ^{1}H NMR (400 MHz, Acetone-D_6) δ = 7.63-7.59 (m, 4 H), 7.45 (d, J = 8 Hz, 2 H), 7.38 (d, J = 16 Hz, 1 H), 7.13 (t, J = 8 Hz, 1 H), 6.98 (s, 1 H), 6.86 (m, 2 H), 6.70 (d, J = 12 Hz, 1 H), 6.16 (s, 1 H), 2.57 (s, 3 H), 1.479 (s, 3 H), 1.43 (s, 3 H); λ_{max} (ε) = 563 nm (82 000 dm^3 mol^{-1} cm^{-1});   HRMS-ESI: m/z: calcd [$C_{26}H_{24}BF_2N_3Na$]$^+$ m/z = 450.1924, found m/z = 450.1930.   For **3b**: ^{1}H NMR (400 MHz, Acetone-D_6) δ = 7.69-7.57 (m, 3 H), 7.45-7.40 (m, 6 H), 6.81 (s, 1 H), 6.75 (d, J = 8 Hz, 2 H), 6.08 (s, 1 H), 2.54 (s, 3 H), 1.46 (s, 3 H), 1.41 (s, 3 H); λ_{max} (ε) = 582 nm (77 000 dm^3 mol^{-1} cm^{-1});   HRMS-ESI: m/z: calcd [$C_{26}H_{24}BF_2N_3Na$]$^+$ m/z = 450.1924, found m/z = 450.1922.

1.3 X-ray structure determination

The X-ray diffraction data were collected on a Bruker Smart Apex CCD diffractometer with graphite monochromated Mo Kα radiation (λ = 0.71073 Å) using the ω–2θ scan mode.   The structure was solved by direct methods and refined on F^2 by full-matrix least-squares methods using SHELX-2000.[S1]   All calculations and molecular graphics were carried out on a computer using the SHELX-2000 program package and ORTEP3 v2.

2b: $C_{26}H_{24}BF_2N_3$; A yellow block-like crystal of the approximate dimensions 0.15 × 0.16 × 0.12 mm^3 was measured.   Monoclinic, space group P2(1)/c, a = 19.318(4) Å, b = 7.0637(14) Å, c = 19.042(4) Å, α = 90, β = 101.007(4), γ = 90, V = 2550.6(9) Å^3, Z = 4, F(000) = 1064.0, ρ = 1.334 Mgm^{-3}, R$_1$ = 0.0890, wR$_2$ = 0.2616, GOF = 1.074, residual electron density between 0.530 and -0.770 eÅ^{-3}.

CCDC No. 1405685 for **2b** containing the supplementary crystallographic data for this paper. These data can be obtained free of charge via www.ccdc.cam.ac.uk/conts/retrieving.html (or from the Cambridge Crystallographic Data Centre, 12 Union Road, Cambridge CB21EZ, UK; fax: (+44)1223–336–033; E-mail: deposit@ccdc.cam.ac.uk).

1.4 Spectroscopic measurements

UV-visible absorption spectra were recorded on a Shimadzu 3000 spectrophotometer.   Fluorescence spectra and the absolute quantum yields (Φ_F) were measured on a Hitachi F-2700 luminescence spectrometer with a 150 W

xenon lamp.   The fluorescence lifetimes of the samples were determined with a Horiba Jobin Yvon Fluorolog-3 spectrofluorimeter, the resolution of the spectrometer is approximately 200 ps.   The goodness of the fit of the single decays as judged by reduced chi-squared (χ_R^2) and the autocorrelation function $C(j)$ of the residuals was always below $\chi_R^2 < 1.2$.   Absorption and emission measurements were carried out in 1×1 cm quartz cuvettes. For all measurements, the temperature was kept constant at (298 ± 2) K.   Dilute solutions with absorbance of less than 0.05 at the excitation wavelength were used for the measurement of fluorescence quantum yields. Rhodamine was used as the standard ($\Phi_F = 0.95$ in ethanol).[S2]   The quantum yield, Φ, was calculated using equation (1):

$$\Phi_{sample}=\Phi_{std}\left[\frac{I\ sample}{I\ std}\right]\left[\frac{A\ std}{A\ sample}\right]\left[\frac{nsample}{nstd}\right]^2 \quad (1)$$

where the *sample* and *std* subscripts denote the sample and standard, respectively, I is the integrated emission intensity, A stands for the absorbance, and n is the refractive index of the solvent.

When the fluorescence decays were monoexponential, the rate constants of radiative (k_f) and nonradiative (k_{nr}) deactivation were calculated from the measured fluorescence quantum yield (Φ_F) and fluorescence lifetime (τ) according to equations (2) and (3):

$$k_r = \Phi_F/\tau \qquad\qquad\qquad (2)$$

$$k_{nr} = (1-\Phi_F)/\tau \qquad\qquad (3)$$

I.5 DFT calculations

The G09W software package was used to carry out DFT geometry optimizations with the B3LYP functional and 6-31G(d) basis sets.[S3]   The same approach was used to calculate the absorption properties based on time-dependent (TD-DFT) method using the B3LYP and CAM-B3LYP functional.

I.6 Cell Culture and Confocal Imaging

Human cervical carcinoma HeLa cell lines were obtained from American Type Culture Collection (ATCC). Hela cells were cultured in Dulbecco's modified Eagle's medium (DMEM) containing 10% fetal bovine serum (FBS),

100 μg mL^{-1} streptomycin and 100 U mL^{-1} penicillin at 37 °C in a humidified incubator. In our experiments, Hela cells were incubated under normoxic (95% air and 5% CO_2) or hypoxic (95% nitrogen and 5% CO_2) conditions at 37 °C for 6 h, and then incubated with 10 μM **1a** for 1 h. Confocal fluorescence imaging studies were performed on a confocal laser scanning microscope (CLSM; TCS SP5, Leica, Germany). Before imaging, the cells were rinsed three times with PBS and kept in phenol red-free culture medium. The cells were excited at 543 nm and the emission was collected from 550 to 650 nm.
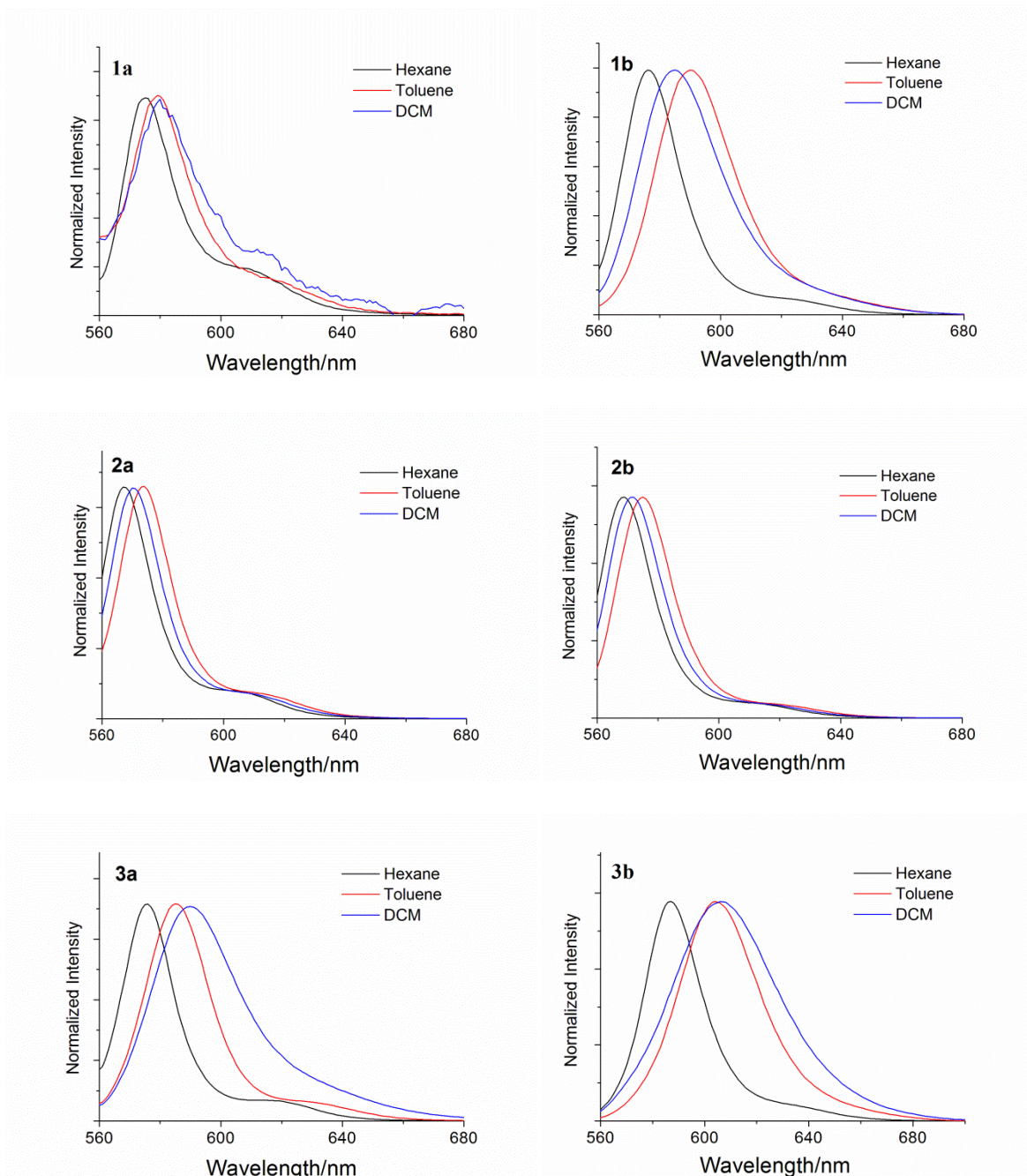
II. Supplementary Figure
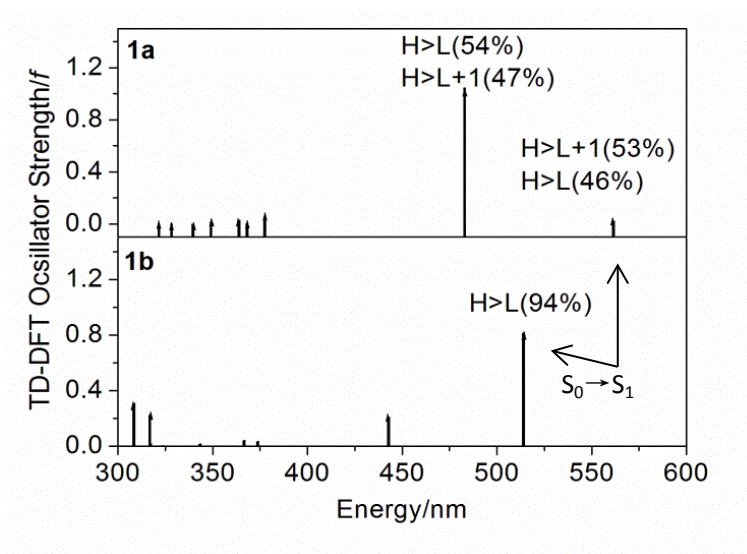
Fig. S1 TD-DFT spectra of **1a** and **1b** based on a DFT geometry optimization using the B3LYP functional with 6-31G(d) basis sets.
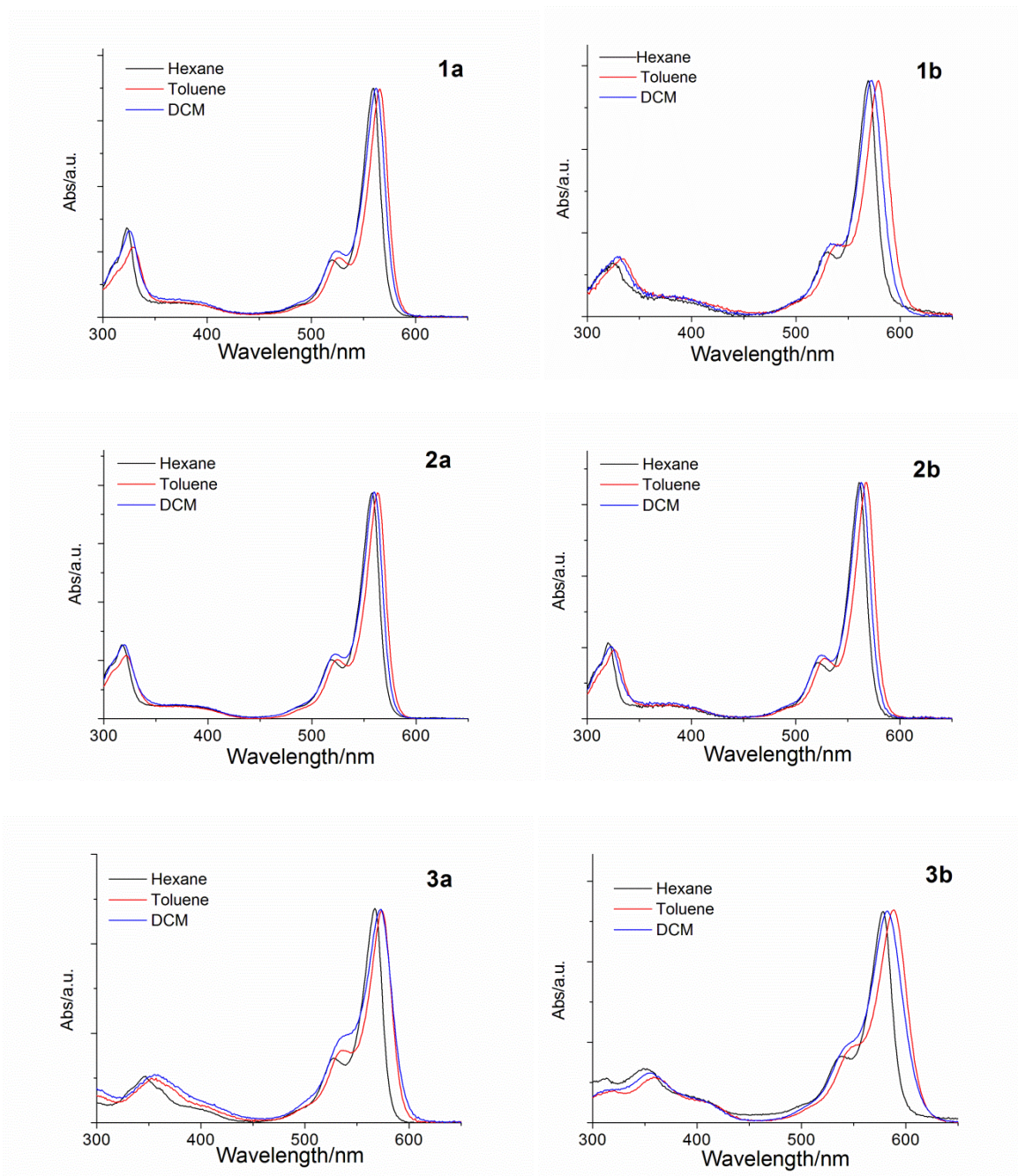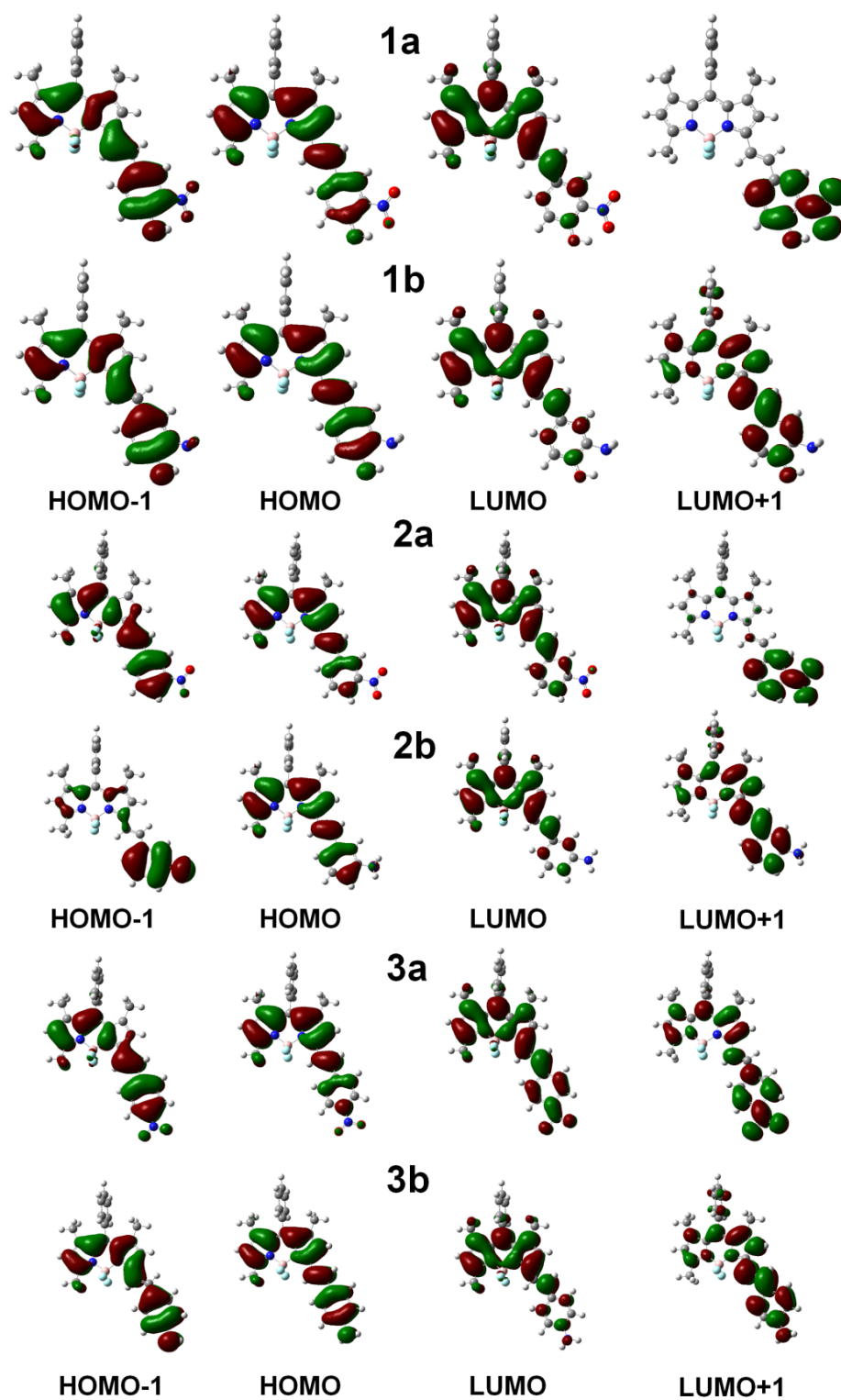
Fig. S2 Absorption spectra of BODIPY **1a**–**3a** and **1b**–**3b** in hexane, toluene and dichloromethane.
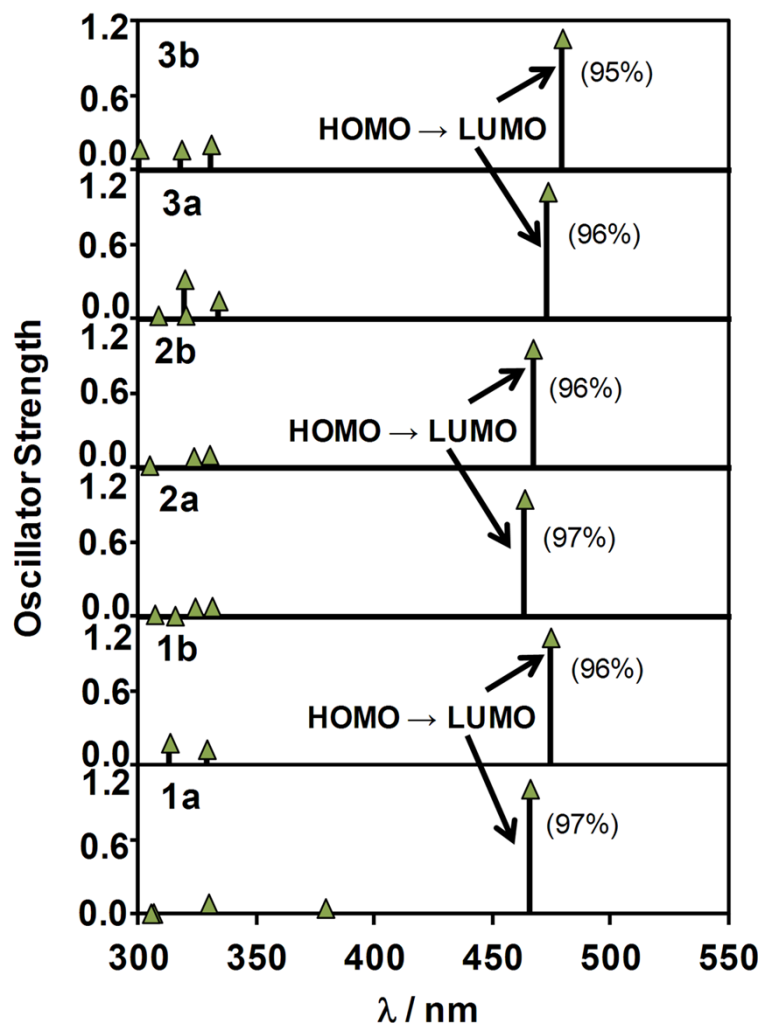
Fig. S3 Emission spectra of BODIPY **1a**–**3a** and **1b**–**3b** in hexane, toluene and dichloromethane.

1a

1b

HOMO-1   HOMO   LUMO   LUMO+1

2a

2b

HOMO-1   HOMO   LUMO   LUMO+1

3a

3b

HOMO-1   HOMO   LUMO   LUMO+1

Fig. S4 Nodal patterns of the frontier π-MOs of **1a**, **1b**, **2a**, **2b**, **3a** and **3b** at an isosurface value of 0.02 a.u.

Fig.S5 TD-DFT spectra for the B3LYP optimized geometries of **1a-3a** and **1b-3b** at the CAM-B3LYP/6-31G(d) level of theory.

III. References

S1   SMART, SAINT, SADABS and SHELXTL, Bruker AXS Inc., Madison, 2000.

S2   A. M. Brouwer, *Pure. Appl. Chem.*, **2011**, *83*, 2213–2228.

S3   Gaussian 09, Revision D.01, M. J. Frisch, G. W. Trucks, H. B. Schlegel, G. E. Scuseria, M. A. Robb, J. R. Cheeseman, G. Scalmani, V. Barone, B. Mennucci, G. A. Petersson, H. Nakatsuji, M. Caricato, X. Li, H. P. Hratchian, A. F. Izmaylov, J. Bloino, G. Zheng, J. L. Sonnenberg, M. Hada, M. Ehara, K. Toyota, R. Fukuda, J. Hasegawa, M. Ishida, T. Nakajima, Y. Honda, O. Kitao, H. Nakai, T. Vreven, J. A. Montgomery, Jr., J. E. Peralta, F. Ogliaro, M. Bearpark, J. J. Heyd, E. Brothers, K. N. Kudin, V. N. Staroverov, R. Kobayashi, J. Normand, K. Raghavachari, A. Rendell, J. C. Burant, S. S. Iyengar, J. Tomasi, M. Cossi, N. Rega, J. M. Millam, M. Klene, J. E. Knox, J. B. Cross, V. Bakken, C. Adamo, J. Jaramillo, R. Gomperts, R. E. Stratmann, O. Yazyev, A. J. Austin, R. Cammi, C. Pomelli, J. W. Ochterski, R. L. Martin, K. Morokuma, V. G. Zakrzewski, G. A. Voth, P. Salvador, J. J. Dannenberg, S. Dapprich, A. D. Daniels, Ö. Farkas, J. B. Foresman, J. V. Ortiz, J. Cioslowski, and D. J. Fox, Gaussian, Inc., Wallingford CT, **2009**.

IV. ¹H NMR

Acetone-d6

Acetone-d6